Computer Simulation of Melt Spinning of Polypropylene Fibers Using a Steady-State Model

Y. C. BHUVANESH and V. B. GUPTA*

Department of Textile Technology, Indian Institute of Technology, Hauz Khas, New Delhi 110 016, India

SYNOPSIS

A mathematical model that includes crystallization in the spinline and the effect of crystallization on the extensional viscosity and the various physical properties of polypropylene has been developed and used to help in identifying the various factors that can affect the spun yarn characteristics. The model is used to simulate effects of spinning parameters on fiber physical properties, temperature, and stresses. The experimental observation of a minimum in density of the spun yarn at high throughput rates, when density is plotted as a function of takeup velocity, has been investigated in some detail. It has been found that all conditions which can substantially affect the rate of cooling and the orientation of the polymer in the spinline, viz, throughput rate, spinning temperature, and spinning speed have an important bearing on the temperature range in which crystallization can take place in the spinline and thus affect the density. It is suggested that in addition to these factors, the formation of different crystal modifications at different spinning speeds could also contribute to the reduction in density of these samples. The model cannot reflect the observation of density changes occurring due to the formation of different crystal modifications. Nevertheless, it can be of use in understanding the effects of various process conditions on the cooling rate and the orientation of the polymer in the spinline. © 1995 John Wiley & Sons, Inc.

INTRODUCTION

The density of fibers spun from nylon 6, nylon 6, 6, and poly(ethylene terephthalate) has been shown to increase with increase in spinning speed,[1-3] apparently because of orientation when the spun fiber is amorphous and orientation and crystallinity when it is semicrystalline. In polypropylene, which is a fast crystallizing polymer, the density is reported to show an increase with increase in spinning speed[4] or a decrease followed by an increase.[5] Jinan et al.[2] obtained experimental data which showed that at spinning temperatures of around 250 to 290°C, the crystallinity of the as-spun yarns gradually decreased with increase in spinning speed, reaching a minimum at a spinning speed of around 600 to 800 m/min before increasing again. The minimum did not appear at lower spinning temperatures and it was observed that in addition to spinning temperature, the melt flow index of the polypropylene sample also affected it. The authors suggested that the competing effects of cooling-dominated crystallization and orientation-induced crystallization were responsible for the minimum. The authors also argued that in the low stress regime in which crystallization is dominated by cooling rates, the spun fiber crystallinity decreases with increasing spinning speed until the orientation effects begin to enhance the rate of crystallization and lead to an increase in the spun fiber crystallinity with further increase in spinning speed. Simulation work carried out by them indicated a similar trend at all spinning temperatures starting from 210 to 290°C.

During our studies on optimization of the spinning conditions for polypropylene and its blends, we observed that for spun polypropylene fibers, all spinning conditions which can substantially affect the rate of cooling and the orientation of the polymer in the spinline, viz, throughput rate, spinning temperature, and spinning speed have an important

* To whom correspondence should be addressed.

Journal of Applied Polymer Science, Vol. 58, 663-674 (1995)
 CCC 0021-8995/95/030663-12

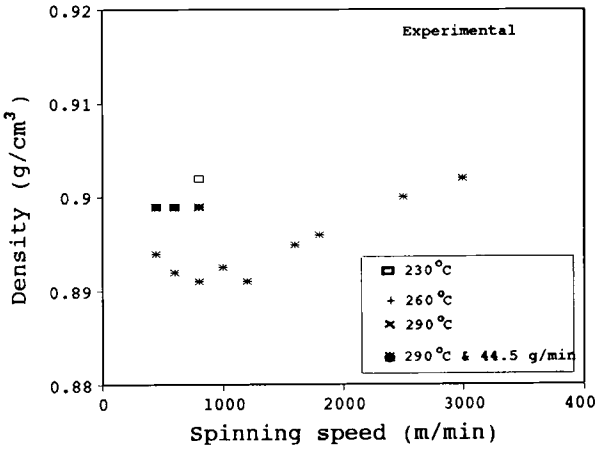

Figure 1 Experimentally obtained density values for samples spun at different spinning temperatures and speeds.

bearing on the temperature range in which crystallization can take place in the spinline and thus affect the density. The minimum in density was observed at a spinning speed in the range of 600 to 800 m/min when the spinning temperature was 290°C and the throughput rate was high. To gain a clearer understanding of this problem, computer simulation of melt spinning of polypropylene was done with an improved model and some very useful results were obtained. They are described and discussed in this paper later. The basic features of the model used for simulation in the present investigation are similar to the ones used by earlier workers.[5-7] Some refinements include the effect of the development of crystallinity on the physical properties of the polymer. The contribution of the amorphous and crystalline phases on the property have been separated to eventually provide a composite value depending on the degree of crystallinity. This can be very helpful in the case of a polymer like polypropylene, which shows a large degree of crystallinity in the spun fiber. The other important feature is the effect of crystallization on the rheological response of the polymer in the spinline. Crystallization results in a large increase in the viscosity of the polymer. To represent this, the viscosity relationship has been modified empirically[9] to include the effect of crystallinity.

BACKGROUND WORK

Fibers Produced and Their Densities

Polypropylene fibers were produced by melt spinning polypropylene chips of melt flow index 20 manufactured by Shell Co. on a pilot scale Fourne SST-1207 melt spinning plant at temperatures of 230, 260, and 290°C at various takeup speeds and throughput rates. The spinneret had 52 holes of 0.3 mm diameter each. The spun sample density was obtained with the help of a Davenport density gradient column prepared from isopropanol and diethyelene glycol. Initially, polypropylene fibers were spun at 450, 600, and 800 m/min at throughput rates of 13.5, 16.2, and 17.5 g/min, respectively, and at temperatures of 230, 260, and 290°C. The experimental results are presented in Figure 1. It was found that the density of the sample spun at 230°C and 800 m/min was higher compared to the other samples (Fig. 1). Another set of samples was spun at 290°C at a throughput of 44.5 g/min and over a range of spinning speeds starting from 450 m/min up to 3000 m/min. As shown in the figure, these samples showed a decrease in density with increase in spinning speed from 450 m/min to about 800 m/min and later increased with further increase in spinning speed. The broad features observed here are similar to those observed by Jinan et al.,[2] but only at very high throughput rates.

Crystallinity and Crystal Structure

The crystallinity of the as-spun samples, obtained at a spinning temperature of 290°C and a constant throughput rate of 44.5 g/min, was measured on a Philips x-ray diffractometer using CuK_α radiation. The I-2θ curves are shown in Figure 2. A qualitative idea of the various crystalline forms in different samples could be gained from these curves. Though a detailed analysis of the crystalline forms was not made, the intensity plots clearly showed that at high speeds the α-monoclinic crystal form predominates while at intermediate speeds, the samples show various combinations of the stable α-form with the less stable pseudohexagonal form. The percentage crystallinity was estimated from these curves by using an amorphous standard[10,11] and fitting it below the I-2θ curves by suitable scaling. This method of measuring crystallinity was suggested by Farrow.[10,11] The crystallinity data are shown in Figure 3. It is interesting to note that like density (Fig. 1), x-ray crystallinity also shows a slight decrease at intermediate windup speeds before increasing again.

MATHEMATICAL MODEL FOR SIMULATION

Introduction to Models Reported in the Literature

Mathematical modeling of the melt spinning process has been largely restricted to noncrystallizing or

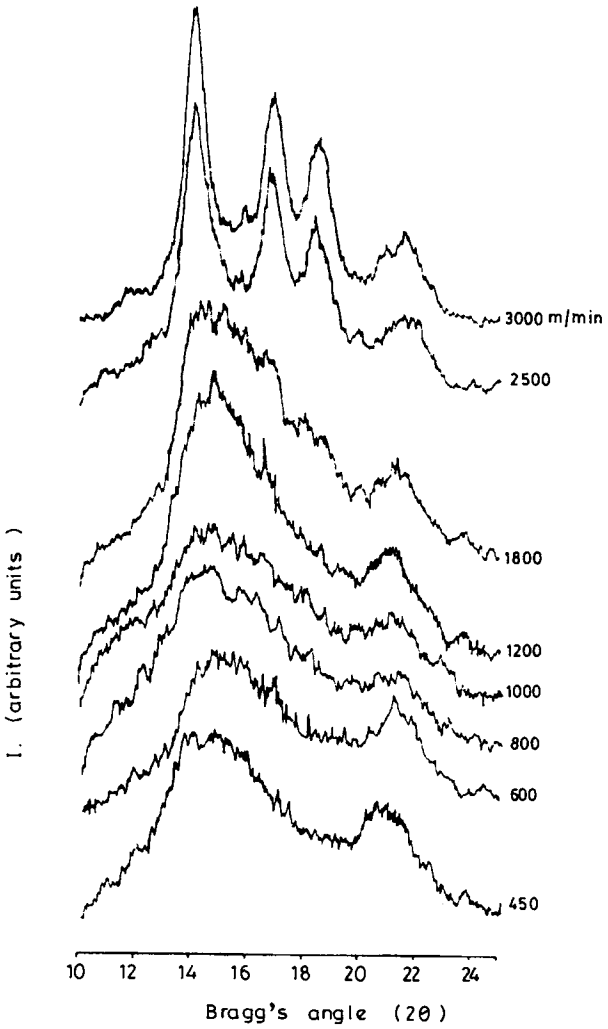

Figure 2 I-2θ curves obtained by x-ray diffraction of samples obtained by spinning at various windup speeds at a constant throughput rate of 44.5 g/min and a spinning temperature of 290°C.

slowly crystallizing systems like atactic polystyrene, poly(ethylene terephthalate), etc.[3-8] The onset of crystallization during melt spinning necessitates the incorporation of some microstructural changes that take place in the spinline into the mathematical model, which can be confirmed by experimental measurements of these features on the spinline itself or on the spun sample. Some attempts have been made to model the melt spinning process with crystallization, which can predict the crystallinity on the spinline by taking into account the effect of amorphous orientation on the rate of crystallization.[2,9,12] It is clearly evident that the effect of orientation in the amorphous phase elements can enhance the rate of crystallization quite substantially. However, the presence of a distribution of molecular orientation and its effect on the crystallization rate and on the resulting orientation in the amorphous phase molecules and the crystallites requires a more sophisticated treatment of the model. Ziabicki and Jarecki[13] propose a molecular theory to explore the role of various molecular features on the resulting crystallization rate. The development of more refined microstructural features like crystallite orientation and other morphological features like chain folding and bundle formation in crystallites is also explored in their work. The process of melt spinning would thus be a complex interplay of polymer rheology, phase change, structure development, heat transfer, aerodynamics, and fluid acceleration. It would be extremely difficult and complicated to incorporate the ideas expounded by Ziabicki and Jarecki into the general continuity, momentum balance, and energy balance equations to arrive at a workable model. Nevertheless, the work is most useful since it attempts to provide an understanding of the evolution of the microstructure and other morphological features in the melt spun fibers. In this article an attempt is made to incorporate some elementary considerations which are necessary to arrive at a model which can predict the development of crystallinity during melt spinning of polypropylene fibers. Polypropylene undergoes rapid crystallization during the process of melt spinning and invariably gives spun filaments which have a high degree of crystallinity.

The Model Used

The mathematical model is briefly presented to understand the implications of some of the features that have been incorporated in the model.

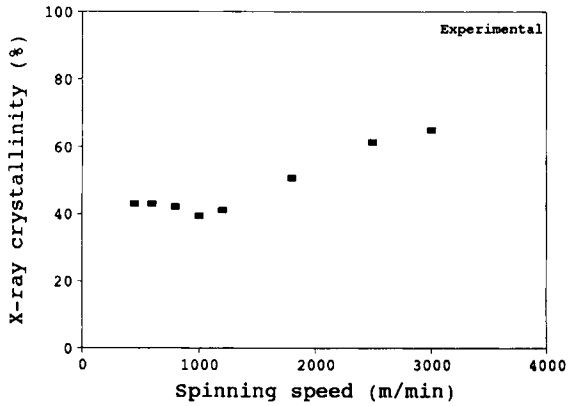

Figure 3 X-ray crystallinity of the samples spun at various windup speeds at a constant throughput rate of 44.5 g/min and a spinning temperature of 290°C.

Differential Equations*

Continuity Equation.

$$W = AV\rho \tag{1}$$

Momentum Balance Equation.

$$\frac{dF_{\text{rheo}}}{dx} = W\frac{dV}{dx} + C_d V^2 \pi D \rho_a / 2 - W\mathcal{g}/V \tag{2}$$

The relationship includes inertial, gravity, and air drag effects.

Energy Balance Equation.

$$\frac{dT}{dx} = \frac{\pi D h (T_a - T)}{W C_p} + \frac{\Delta H}{C_p}\frac{dX}{dx} \tag{3}$$

The effect of crystallization on the heat transfer is also included in the above relationship.

Constitutive Equation.

$$\frac{dV}{dx} = \frac{F_{\text{rheo}}}{A\eta_e} \tag{4}$$

Equation of Amorphous Orientation. The effect of spinline stress on the development of orientation is obtained by using the differentiated stress optical law of Nishiumi,[16] which predicts the amorphous birefringence along the spinline [eq. (5)].

$$\frac{d(\Delta n_a)}{dx} = \frac{C_{\text{op}} E}{V}\frac{dV}{dx} - \frac{E\Delta n_a}{V\eta_e} \tag{5}$$

It incorporates the transient nature of development of orientation in the amorphous regions by representing the relaxation of orientation with the help of a Maxwell model. The development of orientation would then be a function of time and stress (strain rate or velocity gradient). Ziabicki and Jarecki[13] clearly show that in high-speed spinning, the resulting orientation at the end of the spinline can be considerably smaller than the equilibrium value as predicted by the stress-optical law ($\Delta n_a = C_{\text{op}}\sigma$). The stress-optical law is accurate only at very low stresses and hence useful only during slow spinning speeds or in the region close to the spinneret during high-speed spinning. The differentiated stress optical law of Nishiumi introduces the nonlinear nature of the dependence of orientation on the stress.

Equation of Crystallization. The development of crystallinity on the spinline is obtained by using the relationship of Nakamura et al.[23] which is in the differential form with the nonisothermal crystallization rate term being modified to include the effect of orientation also [eq. (6)].

$$\frac{dX}{dt} = n\mathcal{K}(T, f_a)X_\infty\left(1 - \frac{X}{X_\infty}\right) \times \left[\ln\left(\frac{1}{1 - X/X_\infty}\right)\right]^{(n-1)/n} \tag{6}$$

Polypropylene is capable of undergoing crystallization in the spinline even at very low spinning speeds. The role of orientation on the rate of crystallization is itself a very well understood phenomenon. A truly indicative model for the role of orientation on the rate of crystallization can be obtained only by considering individual molecular dynamics.[13] In the absence of a model which can be easily incorporated into the above model, it is practical to take recourse to empirical relationships. Ziabicki suggested the applicability of the following relationship [eq. (7)] for the rate of crystallization under nonisothermal conditions with an additional term included to reflect the effect of amorphous orientation on the rate of crystallization.[14]

$$\mathcal{K}(T, f_a) = \mathcal{K}_{\max}\exp\left[-4\ln(2)\frac{(T - T_{\max})^2}{D_0^2} + Cf_a^2\right] \tag{7}$$

The coefficient C is considered as a constant and reflects the effect of orientation on the rate of crystallization. In the case of polypropylene, the development of crystallization on the spinline is clearly dependent on the temperature and the orientation, which are in turn dependent on the spinline stress. These very factors also determine the morphology of the spun filament. According to Ziabicki and Jarecki,[13] the development of crystallites in the case of a polymer like polypropylene can occur at very low as well as at high stresses. This results in the overall distribution of orientation to be fairly wide and the effective orientation of the crystallites would be somewhat lower. The crystallite orientation would develop independent of the amorphous orientation due to the possibility of rotation of the crystallites and not at the expense of the oriented amorphous phase as in the case of polymers like PET, which undergo very rapid crystallization by neck formation in the spinline. In the case of poly-

* All symbols used in this article are explained in Appendix A.

propylene, according to Ziabicki and Jarecki,[13] the amorphous phase elements can continue to get oriented even after crystallization since the crystallization is not abrupt and the amorphous phase elements which are held between crystallites could continue to get oriented by further deformation of the polymer. This can result in the orientation of the amorphous phase elements to be comparatively higher than in the case of high-speed spun fibers obtained with polymers like PET. These features make the properties of melt spun filaments of polypropylene very different since the most important textile properties like tenacity, elongation to break, initial modulus, heat shrinkage, etc. are very strongly dependent on the degree of crystallinity, crystallite orientation, and amorphous orientation. The picture of spinline crystallization is thus very much different from the models that have been discussed in the literature before. Incorporation of all these polymer-specific features is, however, not easy and hence the model arrived at in this article is much simpler.

Effect of Temperature and Crystallinity on Some Physical Characteristics

The properties of the polymer undergo changes not only as a function of temperature but also as a function of the developing crystallinity along the spinline. The dependence of these properties on crystallinity is quite substantial and the properties show a very large difference, especially, in the case of a polymer like polypropylene which undergoes crystallization to an extent of about 50%. Any model which overlooks this factor might typically underestimate the magnitude of various properties. An attempt is made in this article to choose relationships that take this factor also into account.

Extensional Viscosity (η_e)

The extensional viscosity of the polymer as a function of the polymer intrinsic viscosity and temperature is assumed to follow a semiempirical relationship of the Arrhenius type. The relationship is as follows:[17]

$$\log(\eta_0) = 4.74 \cdot \log([\eta]) + \frac{1.93 \times 10^3}{(T + 273)} - 0.598 \quad (8)$$

$$\eta_e = 3\eta_0 \exp[a(X/X_\infty)^b] \quad (9)$$

Density (ρ)

The density of the amorphous and crystalline fractions is separately evaluated as a function of temperature to finally get the density of the whole by adopting the following set of relationships:[18]

$$\frac{1}{\rho} = \frac{1}{\rho_{am}}(1 - X) + \frac{X}{\rho_c} \quad (10)$$

where

$$\frac{1}{\rho_{am}} = 1.145 + 9.03 \times 10^{-4}T \quad (11)$$

$$\frac{1}{\rho_c} = 1.059 + 4.5 \times 10^{-4}T \quad (12)$$

Specific Heat (C_p)

The specific heat of the polymer is also obtained in the same manner as density and the relationships are as follows:[18]

$$C_p = C_{am}(1 - X) + C_c(X) \quad (13)$$

where

$$C_c = 0.318 + 2.66 \times 10^{-3}T \quad (14)$$

$$C_{am} = 0.502 + 8 \times 10^{-4}T \quad (\text{for } T = 110 \text{ to } 200°C) \quad (15a)$$

$$C_{am} = 0.440 + 2 \times 10^{-3}T \quad (\text{for } T = 0 \text{ to } 110°C) \quad (15b)$$

Parameter Correlations

To calculate the air drag coefficient, Reynolds number, and the heat transfer coefficient, the following relationships have been followed:

Air Drag Coefficient (C_d)

The coefficient of air drag is estimated by using the following relationship of:[19]

$$C_d = 0.68 \times Re^{-0.8} \quad (16)$$

where $Re = VD/\eta_k$ is the Reynolds number.

Heat Transfer Coefficient

The convective heat transfer coefficient with transverse flow of cooling air is computed by using the empirical relationship of Kase and Matsuo.[3]

$$\mathcal{K} = 0.473 \times 10^{-4}(V/A)^{0.334}\left[1 + \left(\frac{8V_a}{V}\right)^2\right]^{0.167} \quad (17)$$

NUMERICAL SOLUTION

The numerical solution of the above set of differential equations requires special care since the various differential equations are nonlinear, implicit, and also stiff. The solution is hence not possible by ordinary single step or multistep methods. The overall stability of the numerical solution of the problem is, however, made quite easy and quick by the use of Radau method. A Radau routine of the fifth order is applied for the solution of the above system of equations.[22]

Data Used

The simulation has been carried out with the following set of data:

$D(x = 0) = 0.03$ cm
$T(x = 0) = 230$, 260, and 290°C
$V_L = 500$, 1000, 1500, 2000, 2500, and 3000 m/min
$W = 0.9$ g/min
$V_a = 80$ cm/min
$T_a = 25$°C

Boundary Conditions

The following boundary conditions have been used for the solution of the differential equations

$$F_{\text{rheo}}(x = 0) = F_{\text{initial}} \quad \text{(initial force)}$$
$$T\,(x = 0) = T_0 \quad \text{(spinning temperature)}$$
$$D\,(x = 0) = 0.03 \text{ cm} \quad \text{(spinneret diameter)}$$
$$X\,(x = 0) = 0.0$$
$$\Delta n_a\,(x = 0) = 0.0$$
$$V\,(x = 0) = V_0 \quad \text{(filament velocity at spinneret)}$$
$$V\,(x = L) = V_L \quad \text{(filament velocity at takeup)}$$

Table I Values of Important Physical Parameters Used in Carrying out the Computer-Based Predictions

Constant	Value Used	Authors/Source Reference No.
T_m	180°C	14, 15
$T_{\max}$	65°C	14, 15
D_0	60°C	14, 15
$\mathcal{K}_{\max}$	0.55 s^{-1}	14, 15
ΔH	20.1 cal/g	20
X_∞	0.5	12
C	40×10^3	Assumed
Δ^0_{am}	0.0468	21
Δ^0_c	0.0331	21
n	1	Assumed
C_{op}	0.089×10^{-9} cm^2/dyn	8
E	2×10^6 dyn/cm^2	Our data
a	3.0	Assumed
b	12	Assumed

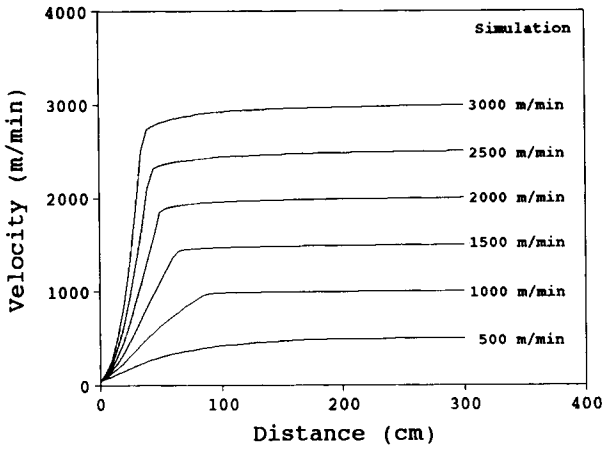

Figure 4 Computer predictions of filament velocity as a function of distance from the spinneret exit at various spinning speeds obtained for a spinning temperature of 230°C.

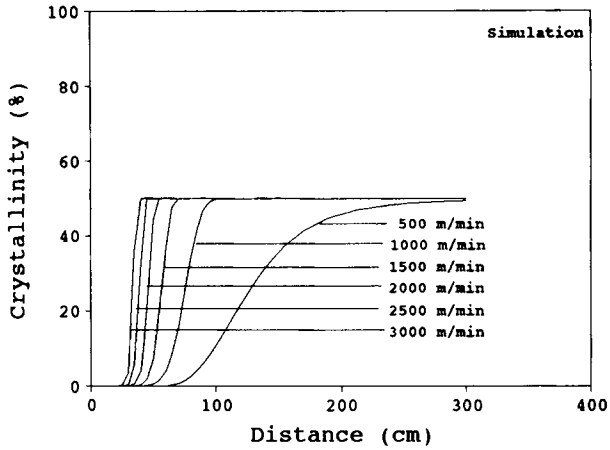

Figure 6 Computer predictions of crystallinity developed in the filament in the spinline at various spinning speeds and a temperature of 230°C.

The takeup point was considered to be located at a distance of 3 m from the spinneret exit.

RESULTS AND DISCUSSION

Prediction of Spinline Parameters

For the numerical solution of the set of differential equations [eqs. (1–7)] in conjunction with the relationships that reflect the properties of the polymer [eqs. (8–15)] and the relationships required for the evaluation of the various parameters [eqs. (16–18)], it is necessary to take appropriate values for some of the physical parameters that will be used in the solution. A list of the parameters used and the corresponding values are tabulated in Table I. The values of coefficient, C, and of the Avrami index, n, were taken to be 40×10^3 and unity, respectively. The value of the coefficient, C, was obtained by carrying out a number of trial calculations. The values used for both C and n are consistent with those used in the literature.[2,9,12] Data obtained by simulation at a temperature of 230°C for velocity, temperature, crystallinity, spinline stress, amorphous birefringence, and total birefringence are shown in Figures 4 to 9. The velocity (Fig. 4) reaches close to its limiting value (V_L) in a very short distance from the spinneret. This is apparently due to the rapid cooling that takes place in the spinline due to the presence of the transverse cooling air and also due to the in-

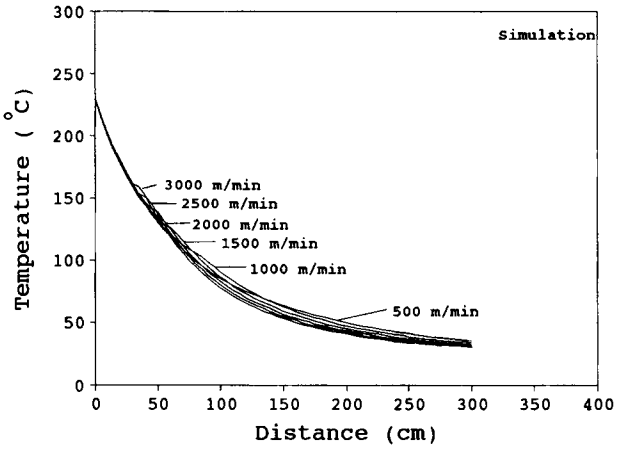

Figure 5 Computer predictions of filament surface temperature as a function of distance from the spinneret exit at various spinning speeds and a temperature of 230°C.

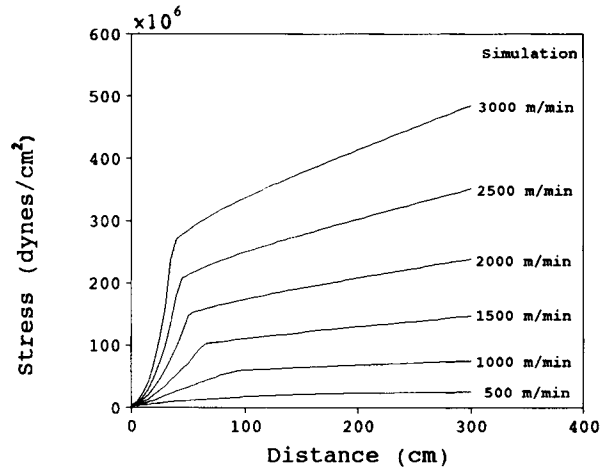

Figure 7 Spinline stress predicted by the model at various spinning speeds and temperatures and a temperature of 230°C.

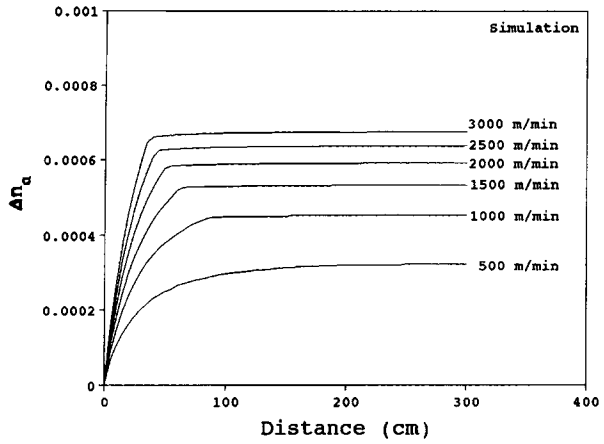

Figure 8 Amorphous birefringence (Δn_a) developed as a function of spinline distance as predicted by the model at a spinning temperature of 230°C and at various spinning speeds.

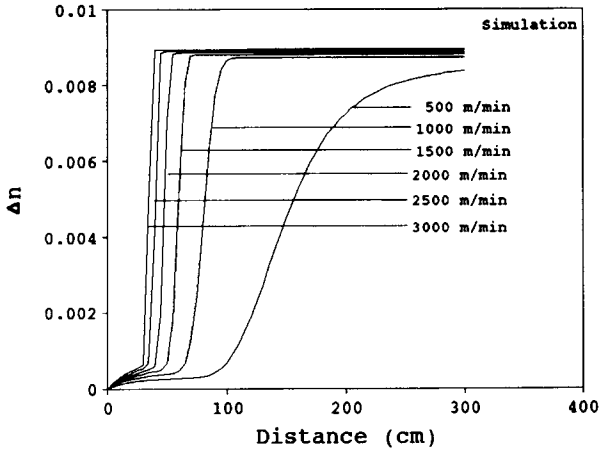

Figure 9 Total birefringence (Δn) along the spinline plotted for various spinning speeds and a temperature of 230°C as obtained by computer predictions.

troduction of the crystallinity dependence of viscosity in the relationship for viscosity. This results in an enhancement of the viscosity by the onset of crystallization and hence most of the deformation has to take place in the region before the onset of crystallization. The temperature curve (Fig. 5) shows the presence of a very mild plateau or bulge in the region of the spinline where the crystallization is occurring. This observation is very different from that observed during spinning of PET at very high speeds. This can be explained in terms of the rate of crystallization, which in the case of polypropylene is gradual, unlike in the case of PET for which crystallization is rather abrupt and is accompanied by the observation of a neck in the spinline.[1] At 500 m/min (Fig. 6), the crystallization takes place in a distance up to about 250 cm from the spinneret. However, at 3000 m/min, the crystallization is over within 35 cm from the spinneret. The rapid rate of crystallization due to the increased spinline stress (Fig. 7) or amorphous orientation (Fig. 8) at higher speeds is clearly brought out by the model. The orientation of the amorphous phase (Fig. 8) increases before stabilizing at a point where the filament begins to show crystallinity. The birefringence plots (Fig. 9) show three distinct regions. In the initial region, which is immediately after the spinneret, the rise in birefringence is almost entirely due to the amorphous contribution. Crystallization has not yet set in either due to insufficient supercooling or orientation. This region is followed by a region of rapid rise in birefringence due to crystallization. The birefringence stabilizes once the crystallization is complete.

The spinline stress at the takeup increases with takeup velocity (Fig. 10) at all temperatures. At a higher temperature of spinning, the stress at takeup is lowered. This is also reflected in the amorphous birefringence at takeup (Fig. 11). At higher spinning temperatures of 260 and 290°C, the birefringence (Fig. 12) and crystallinity (Fig. 13) are somewhat lower than the maximum crystallinity in the case of 500 m/min.

Temperature of Initiation of Crystallization

The temperature at which crystallization is initiated increases with the increase in spinning speed (Fig. 14). This can be understood on the basis of the

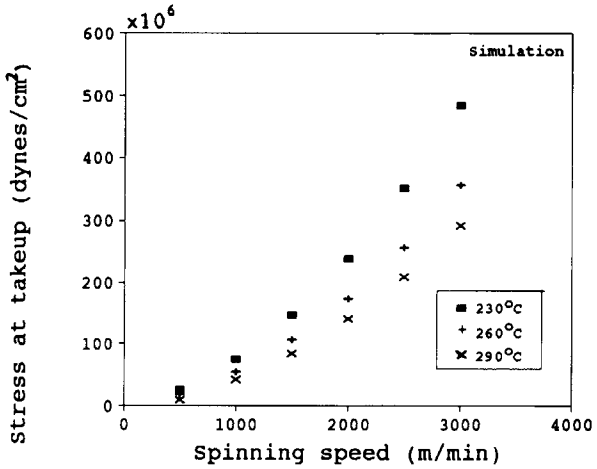

Figure 10 Variation of stress at the takeup point obtained from the model predictions as a function of spinning speed at various spinning temperatures.

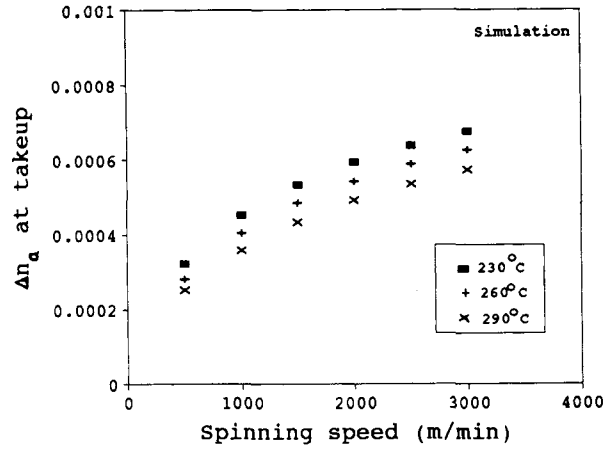

Figure 11 Amorphous birefringence at the takeup point plotted as a function of spinning speed at various spinning temperatures obtained by the model.

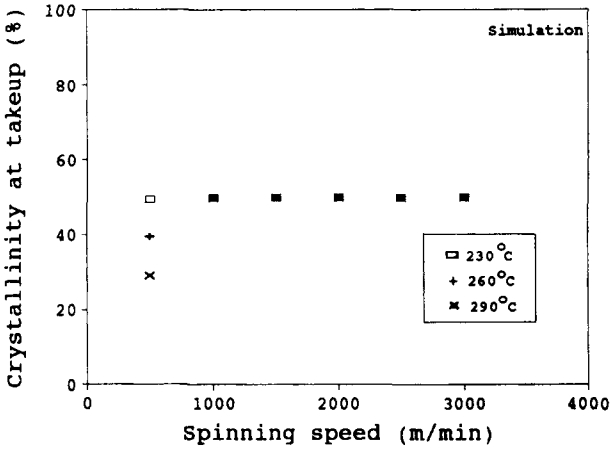

Figure 13 Crystallinity at the takeup point predicted by the model at various spinning speeds and temperatures.

spinline stress (Fig. 15) and amorphous orientation (Fig. 16) reached prior to the onset of crystallization. The higher orientation in the amorphous phase, which itself follows from the higher spinline stress, makes it possible for the crystallization to occur at a higher temperature. Referring to Figure 14, it can be observed that the temperature at which crystallization is initiated is shifted toward lower temperatures when the spinning temperature is raised from 230 to 260 and 290°C. This can be understood in terms of the amorphous birefringence at which the crystallization is initiated (Fig. 16). The amorphous birefringence at which crystallization is initiated at higher spinning temperatures is lower and this ensures that the crystallization at higher spinning temperatures occurs at higher levels of supercooling.

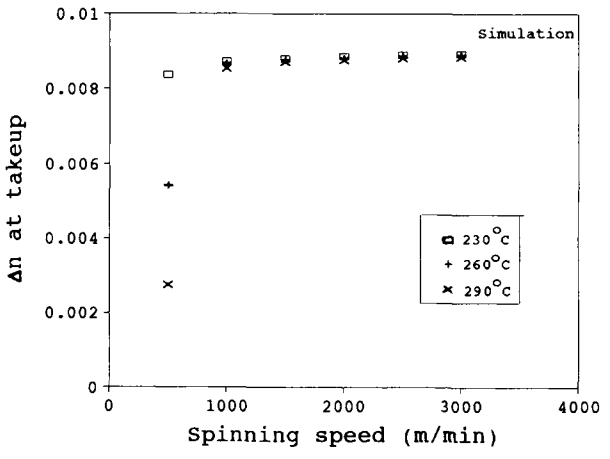

Figure 12 Total birefringence at the takeup point at various spinning speeds and temperatures as predicted by the model.

The temperature of initiation of the crystallization can also be used as an important indicator of the nature of crystal modification resulting from a particular spinning process. From Figure 14, it can be seen that at all spinning temperatures and spinning speeds, the crystallization is initiated at temperatures above 100°C. In a quiescent state experiment, the high temperature x-ray work showed that initiation of crystallization is about 100°C and above.[24]

Crystallinity and Its Dependence on Spinning Speed

The results obtained by simulation (Fig. 13) show that the crystallinity is lower (42%) at 500 m/min with a spinning temperature of 290°C. At higher spinning speeds, the crystallinity obtained is equal to the maximum value (50%) and does not show

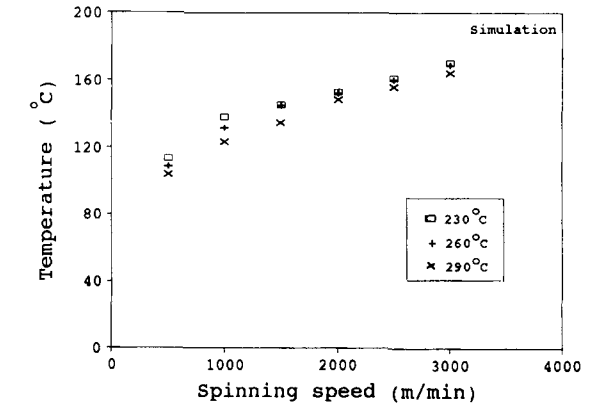

Figure 14 Crystallization start temperature predicted by the model as various spinning speeds and temperatures.

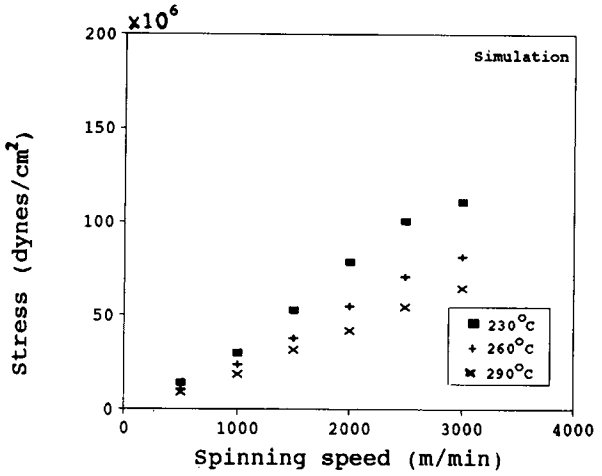

Figure 15 Spinline stress at the point of initiation of crystallization as predicted by the model under various conditions of spinning speed and temperature.

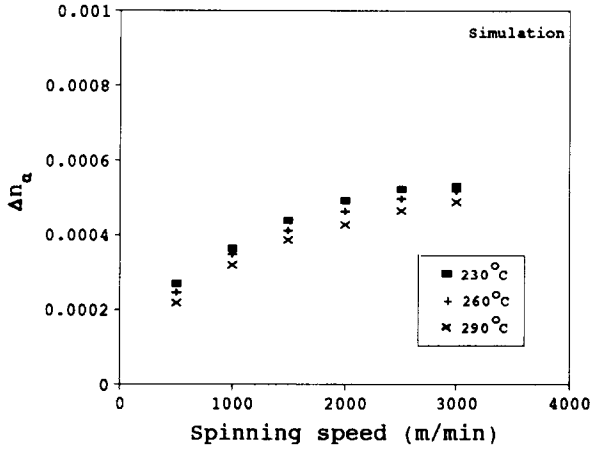

Figure 16 Amorphous birefringence at the point of initiation of crystallization as predicted by the model under various conditions of spinning speed and temperature.

any change. The experimental data show such behavior when spinning is carried out at low throughput rates (Fig. 1). At higher throughput rates (44.5 g/min), however, the density shows a minimum when plotted as a function of spinning speed. The drop in density could be due to two possible causes. First, the reduction in the crystallinity of the spun samples as observed experimentally (Fig. 3) could be attributed to rapid quenching and also the absence of orientation-induced crystallization. Second, the various crystal modifications formed in the samples spun at different spinning speeds, as observed in Figure 2 and described previously, could lead to a drop in density. Crystallization occurring at temperatures lower than 110°C can result[25,26] in the formation of the less stable pseudohexagonal form with crystal density of 0.916 g/cm^3, which can undergo transformation to the stabler modification (monoclinic α form, crystal density 0.946 g/cm^3) at temperatures above 110°C.[25,26] Spinning conditions, which can result in the crystallization taking place at much higher temperatures (above 110°C), can lead to the formation of the stabler α-modification. At very low spinning speeds, the quench rate is lowest and can result in the crystallization occurring at high temperatures and giving rise to a predominantly monoclinic form. Orientation-induced crystallization can also increase the temperature of crystallization and lead to the formation of monoclinic crystals. In the region of intermediate spinning speeds, due to a faster rate of cooling and also to the absence of orientation-induced crystallization, it is probable that a substantial part of the crystallization is occurring below 110°C and could lead to the formation of the pseudohexagonal form.

The simulation model, however, is not capable of reflecting density changes which result from different crystal modifications. The observation of the pseudohexagonal crystal structure and its effect on the overall density of the spun sample cannot be reflected in the model that has been used in this article. The competing effects of cooling dominated crystallization and orientation induced crystallization can be introduced in the model by making some changes in the values of the parameters used in the model; by using a value of 2 instead of 0.55 s^{-1} for the maximum crystallization rate constant under isothermal conditions ($\mathcal{K}_{max}$) and 2.9 $\times$ 10^3 for the coefficient of orientation-induced crystallization term (C). Figure 17 shows a minimum in the crystallinity as a function of spinning speed at different

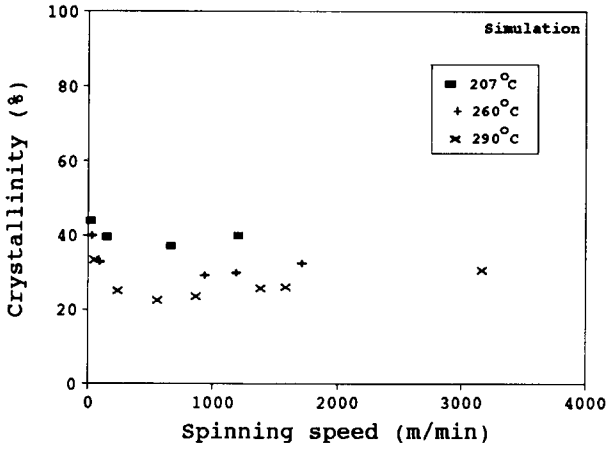

Figure 17 Crystallinity dependence at the takeup point on the spinning speed at various temperatures with the changed parameters of $\mathcal{K}_{max}$ = 2 s^{-1} and C = 2.9 $\times$ 10^3.

spinning temperatures. The extent of drop in crystallinity before beginning to rise reduces as the spinning temperature is also lowered. This feature is also similar to the trend observed by Jinan et al.[2] in their simulation results.

Effect of Throughput Rate

Increasing throughput rates can also lower the rate of quenching and can lead to a reduction of the spun fiber density (Fig. 18). The dependence of density at any spinning speed is substantially affected by the throughput rate since it can alter the rate of quenching. Figure 18 shows very clearly the resulting drop in density due to an enhancement of the throughput rate during spinning at a takeup speed of 800 m/min. A similar conclusion can be drawn at other spinning speeds also by examining the data plotted in Figure 1, which show that increase in throughput rates can invariably result in a lower value of density of the spun sample up to a certain limit irrespective of the spinning temperature. This drop in density itself can be explained on the basis of the formation of the various crystal modifications depending on the temperature of crystallization. In the samples spun at low throughput rates, the crystal modification was observed to have a predominantly monoclinic form while at the highest throughput rate, the spun sample showed a predominantly pseudohexagonal form of crystal modification with samples produced at intermediate throughput rates showing a gradual reduction of the monoclinic form.

CONCLUSIONS

The variation of the density of the sample as a function of takeup velocity at the higher throughput rate of 44.5 g/min shows a minimum at around 800 to 1000 m/min in the samples spun at a temperature of 290°C. The location of the dip can vary depending on the spinning temperature and the actual throughput rates. The drop in density itself can be explained on the basis of two factors. First, the formation of different crystal modifications during crystallization like the stabler monoclinic form or the metastable pseudohexagonal form, and second, due to a reduction in the crystallinity of the spun sample. The reduction is possible if the quench rate of the extruded filaments is higher and the contribution to crystallinity from the orientation effects is not substantial. The temperature at which crystallization is occurring has an important influence on the formation of various crystal modifications

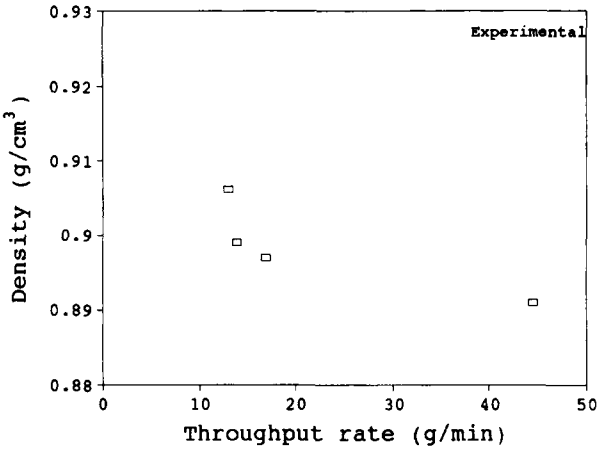

Figure 18 Variation of the experimentally determined density of the samples spun at different throughput rates and at a temperature of 260°C.

observed in spun samples. The model used for simulation in this article, although not capable of reflecting all these features, can nevertheless be used as a useful tool in anticipating the effect of any change in processing conditions, especially its effect on the rate of cooling and the likely temperature range in which crystallization could be taking place. It may be concluded that all conditions which affect the rate of cooling and the orientation of the polymer in the spinline have an important bearing on the temperature at which crystallization occurs. This in turn can lead to the observation of different crystal modifications which can affect the overall structure of the spun fiber and also its density. The spinning temperature, throughput rate, and the takeup velocity turn out to be the most important technological parameters that can significantly affect the spun fiber characteristics.

APPENDIX A

Nomenclature

a	coefficient of the crystalline fraction in the term for the effect of crystalline fraction on the extensional viscosity
A	area of cross section of the filament along the spinline (cm^2)
b	exponent of the crystalline fraction in the term for the effect of crystalline fraction on the extensional viscosity
C	coefficient of orientation term in the crystallization rate constant equation
C_{am}	specific heat of the amorphous fraction in the filament (cal/g)

C_c specific heat of crystalline fraction (cal/g)
C_d air drag coefficient
C_{op} stress optical coefficient (cm^2/dyn)
C_p specific heat of the polymer (cal/g)
D diameter of the filament along the spinline (cm)
D_0 crystallization rate half width (°C)
E modulus of the filament (dyn/cm^2)
f_{am} Herman's orientation factor of amorphous fraction
f_c Herman's orientation factor of crystalline fraction
$F_{airdrag}$ air drag force exerted on the running filament (dyn)
$F_{inertial}$ inertial contribution to the spinline tension (dyn)
$F_{gravity}$ gravity contribution to spinline tension (dyn)
F_{rheo} rheological force (dyn)
g gravitation constant (cm/s^2)
h convective heat transfer coefficient (cal/g-cm^2-°C)
K crystallization rate constant (s^{-1})
K_{max} maximum crystallization rate constant under isothermal and quiescent conditions (s^{-1})
n Avrami exponent
Re Reynolds number
σ spinline stress (dyn/cm^2)
T temperature of the filament along the spinline (°C)
V velocity of the filament along the spinline (cm/s)
V_a velocity of transverse cooling air (cm/s)
W polymer throughput per capillary (g/s)
X fraction of crystallization
X_∞ maximum fraction of crystallization
x distance along the spinline from the spinneret (cm)
Δ°_{am} intrinsic amorphous birefringence
Δ°_c intrinsic crystalline birefringence
ΔH heat of fusion of the polymer (cal/g)
Δn total birefringence
Δn_a birefringence of amorphous fraction
$[\eta]$ intrinsic viscosity of polymer (dl/g/mol)
η_e extensional viscosity of the polymer (P)
η_k kinematic viscosity of the transverse cooling air (P-cm^3/g)
η_0 shear viscosity of the polymer at very low shear rates (P)
ρ density of the filament (g/cm^3)
ρ_a density of the cooling air (g/cm^3)
ρ_{am} density of the amorphous fraction (g/cm^3)
ρ_c density of the crystalline fraction (g/cm^3)

REFERENCES

1. J. Shimizu, N. Okui, and T. Kikutani, in *High Speed Fibre Spinning*, A. Ziabicki and H. Kawai, Eds., Wiley Interscience, New York, 1985, p. 173.
2. C. Jinan, T. Kikutani, A. Takaku, and J. Shimizu, *J. Appl. Polym. Sci.*, **37**, 2683 (1989).
3. S. Kase and T. Matsuo, *J. Polym. Sci.*, **3A**, 2541 (1965).
4. S. Kase and T. Matsuo, *J. Polym. Sci.*, **11**, 251 (1967).
5. D. K. Gagon and M. M. Denn, *Polym. Eng. Sci.*, **21**, 884 (1981).
6. H. H. George, *Polym. Eng. Sci.*, **22**, 291 (1982).
7. A. Dutta and V. M. Nadkarni, *Text Res. J.*, **54**, 35 (1984).
8. Y. C. Bhuvanesh and V. B. Gupta, *Indian J. Fibre Text Res.*, **15**, 145 (1990).
9. K. F. Zieminski and J. E. Spruiell, *J. Appl. Polym. Sci.*, **35**, 2223 (1988).
10. G. Farrow, *Polymer*, **1**, 520 (1961).
11. G. Farrow, *J. Appl. Polym. Sci.*, **9**, 1227 (1965).
12. K. Katayama and M. G. Yoon, in *High Speed Fibre Spinning*, A. Ziabicki and H. Kawai, Eds., Wiley Interscience, New York, 1985, p. 207.
13. A. Ziabicki and L. Jarecki, in *High Speed Fibre Spinning*, A. Ziabicki and H. Kawai, Eds., Wiley Interscience, New York, 1985, p. 225.
14. A. Ziabicki, *Fundamentals of Fibre Formation*, Wiley, New York, 1976, p. 111.
15. J. H. Magill, *Polymer*, **3**, 35 (1962).
16. S. Nishiumi, *Sen-I Kikai Gakkaishi*, **18**, 1974 (1965).
17. Y. Sano, K. Orii, and N. Yamada, *Sen-I Gakkaishi*, **24**, 147 (1968).
18. N. Yamada, Y. Sano, and T. Nanbu, *Sen-I Gakkaishi*, **24**, 197 (1966).
19. Y. Sano and K. Orii, *Sen-I Gakkaishi*, **24**, 212 (1968).
20. K. Kamide and K. Nakamura, *Sen-I Gakkaishi*, **24**, 486 (1968).
21. H. Takahara, H. Kawai, and T. Yamada, *Sen-I Gakkaishi*, **24**, 219 (1968).
22. E. Hairer and G. Wanner, *Solving Ordinary Differential Equations II, Stiff and Differential-Algebraic Problems*, Springer Series in Computational Mathematics, Springer-Verlag, Berlin, 1991.
23. K. Nakamura, K. Katayama, and T. Amano, *J. Appl. Polym. Sci.*, **17**, 1031 (1973).
24. Y. C. Bhuvanesh and V. B. Gupta, *Polymer*, to appear.
25. O. Ishizuka, *Sen-I Gakkaishi*, **18**, 198 (1962).
26. R. S. Stein, *J. Polym. Sci.*, **A-3**, 1741 (1965).

Received February 7, 1995
Accepted April 12, 1995